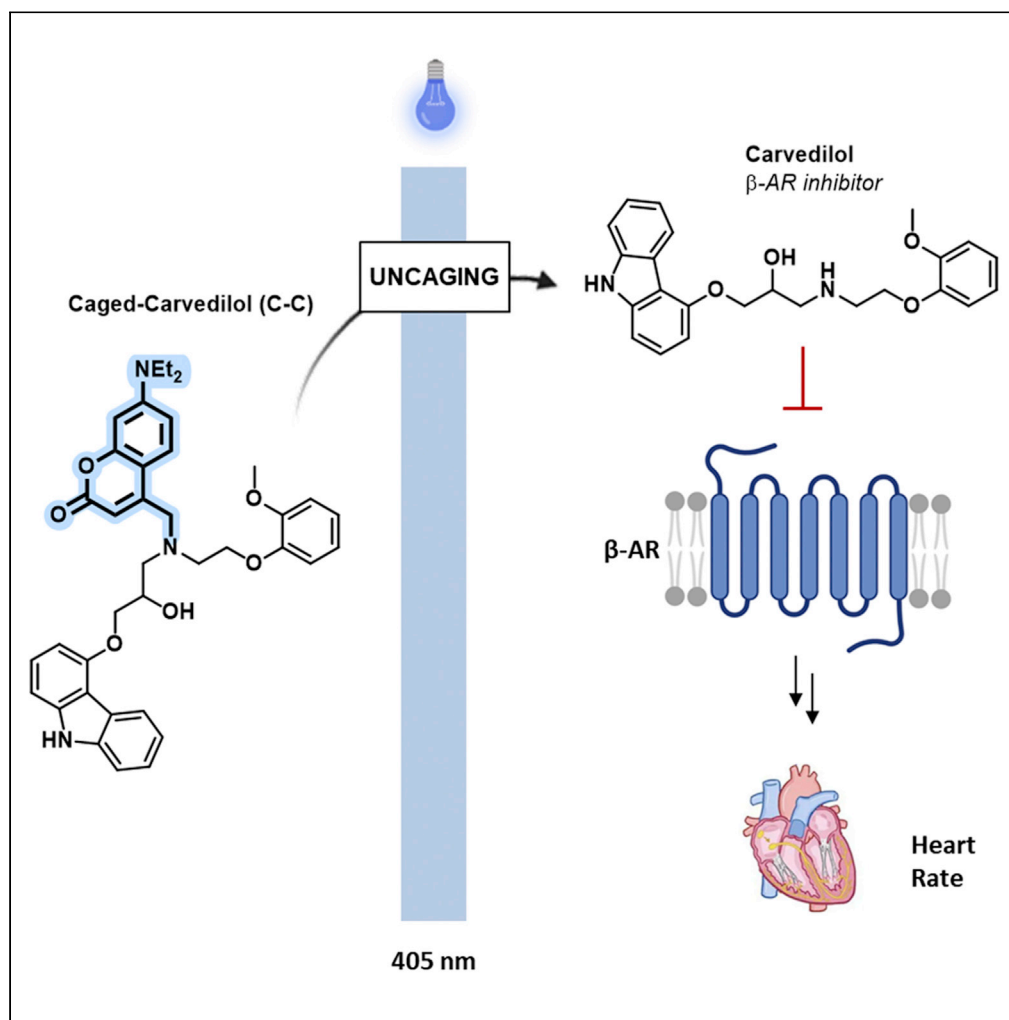## Article

Caged-carvedilol as a new tool for visible-light photopharmacology of β-adrenoceptors in native tissues

Anna Duran-Corbera, Joan Font, Melissa Faria, ..., Antonio Rodriguez-Sinovas, Amadeu Llebaria, Xavier Rovira

amadeu.llebaria@iqac.csic.es (A.L.)
Xavier.rovira@iqac.csic.es (X.R.)

Highlights

We report a diffusible caged antagonist based on the beta blocker carvedilol (C-C)

Carvedilol release from C-C is produced by light on the visible range (405 nm)

Light-dependent effects are assessed in cells, mice hearts, and zebrafish larvae

Physiological processes can be regulated by C-C and light (heart rate and behavior)

iScience

Article

Caged-carvedilol as a new tool for visible-light photopharmacology of β-adrenoceptors in native tissues

Anna Duran-Corbera,[1] Joan Font,[1] Melissa Faria,[2] Eva Prats,[3] Marta Consegal,[4,5,6] Juanlo Catena,[7] Lourdes Muñoz,[7] Demetrio Raldua,[2] Antonio Rodriguez-Sinovas,[4,5,6] Amadeu Llebaria,[1,*] and Xavier Rovira[1,8,9,*]

SUMMARY

Adrenoceptors are G protein-coupled receptors involved in a large variety of physiological processes, also under pathological conditions. This is due in large part to their ubiquitous expression in the body exerting numerous essential functions. Therefore, the possibility to control their activity with high spatial and temporal precision would constitute a valuable research tool. In this study, we present a caged version of the approved non-selective β-adrenoceptor antagonist carvedilol, synthesized by alkylation of its secondary amine with a coumarin derivative. Introducing this photo-removable group abolished carvedilol physiological effects in cell cultures, mouse isolated perfused hearts and living zebrafish larvae. Only after visible light application, carvedilol was released and the different physiological systems were pharmacologically modulated in a similar manner as the control drug. This research provides a new photopharmacological tool for a wide range of research applications that may help in the development of future precise therapies.

INTRODUCTION

Adrenoceptors are class A G protein-coupled receptors (GPCR) divided in three subtypes named α_1, α_2 and β (Altosaar et al., 2019). The presence of these receptors in different organs and their key role in many important physiological functions has appointed them as classical pharmacological targets (Perez, 2005). Indeed, there are a number of approved drugs targeting adrenoceptors for the treatment of several conditions, such as asthma or anxiety, among many others. (Altosaar et al., 2019) In particular, the use of β-adrenoceptor (β-AR) antagonists to treat cardiovascular diseases is one of the most common pharmacological applications of these targets. (Perez, 2005; Wachter and Gilbert, 2012) Moreover, beyond their common applications in the treatment of cardiovascular diseases, new uses for β-AR agonists and beta blockers are being proposed. (Velmurugan et al., 2019) Of note, two beta blockers, metoprolol, and albuterol, are among the ten most prescribed drugs in the United States even though their discovery was almost 40 years ago. Moreover, propranolol, atenolol, and carvedilol are also among the top 50. These data highlight the relevance of adrenoceptors in general, and β-AR in particular as drug targets for a number of diseases.

Carvedilol is a non-selective beta blocker, mainly targeting β_1-and β_2-adrenoceptors (β_1-AR and β_2-AR) (Baker, 2005). Nevertheless, it has also been described as an α_1-adrenoceptor antagonist, which provides this drug with particular hypotensive effects (Koshimizu, 2004; Wong et al., 2015). Furthermore, it has been recently demonstrated that carvedilol possesses a unique mechanism of action because it can stimulate β-arrestin signaling and promote receptor internalization while blocking Gs protein activation, a GPCR pharmacological property that has been called biased agonism or functional selectivity (Wisler et al., 2007). Special efficacy for the treatment of heart failure has been attributed to these particular features, (Wang et al., 2021) providing carvedilol with additional therapeutic potential which is worth exploring. Indeed, beyond cardiovascular diseases, new applications based on the interesting pharmacological profile of this beta blocker are emerging, such as enhancement of skeletal muscle contractility (Kim et al., 2020). Altogether, makes carvedilol an especially interesting drug for physiological and pharmacological research to elucidate the role of adrenoceptors in specific tissues and organs.

Photopharmacology is an emerging research field with the main objective of precisely controlling native biological systems in a spatiotemporally restricted manner.(Fuchter, 2020; Hüll et al., 2018; Lerch et al.,

2016) To that aim, light-regulated molecules are developed allowing a selective modulation of the target. These light-sensitive molecules can be reversible or irreversible, which constitute the two main strategies followed in GPCR photopharmacology (Ricart-Ortega et al., 2019). Reversible photoswitches are usually developed by introducing a photochromic moiety in the structure of known ligands. A number of photoswitches have been developed to successfully regulate the activation state of several receptors with light (Hüll et al., 2018; Ricart-Ortega et al., 2019). Many class A GPCRs have been targeted using synthetic photoswitches (Agnetta et al., 2017; Bahamonde et al., 2014; Broichhagen et al., 2015; Donthamsetti et al., 2017; Frank et al., 2017; Gómez-Santacana et al., 2018; Hauwert et al., 2018; Hüll et al., 2021; Morstein et al., 2020; Schönberger and Trauner, 2014; Westphal et al., 2017) among which, very recently, also β_1-AR(Duran-Corbera et al., 2022) and β_2-AR (Duran-Corbera et al., 2020). On the other hand, irreversible molecules named caged compounds are produced by adding a photocleavable group to a known active molecule, which hampers the formation of the ligand-receptor complex, thus rendering the molecule inactive (Tapia et al., 2021; Vickerman et al., 2021). On illumination, the photoprotecting group (PPG) is photolyzed and the active compound is locally and irreversibly released from the inactive precursor. This approach that emerged in the late seventies (Ellis-Davies, 2020) and has been widely developed in the 21st century, is focusing nowadays on the search for photocages operating at visible light wavelengths (Josa-Culleré and Llebaria, 2021). The caging strategy has also been applied to target several GPCRs (Banghart et al., 2013, 2018; Banghart and Sabatini, 2012; Callaway and Katz, 1993; Ellis-Davies, 2007; Font et al., 2017; López-Cano et al., 2021; Taura et al., 2018; Todde et al., 2000), including β-AR (Muralidharan and Nerbonne, 1995). Caged compounds targeting β-AR have been used in a variety of research studies, taking advantage of their lipophilic nature and their selective light-dependent activation properties. For instance, cell-permeant caged isoproterenol analogues have been used to study intracellular β-adrenoceptors present in the nuclei (Vaniotis et al., 2013). In another study, the beta blocker timolol was linked to the polymer of contact lenses via a photocleavable caged cross-linker (Mu et al., 2018). In this interesting approach, the drug was released on passive exposures to natural daylight. Furthermore, the authors demonstrated that these functionalized lenses may have applications for glaucoma patients, where the intraocular pressure was reduced in a controlled manner, for longer times with lower concentrations, which may help reduce undesired effects of current treatments. This study highlights the great potential of drug caging strategy targeting β-AR for therapeutic applications.

Despite the wide use of beta blockers for more than half a century (Stapleton, 1997), their mechanism of action is not completely understood and new therapeutic applications for these drugs are still being proposed (Filoni et al., 2021; Gelosa et al., 2020; Peixoto et al., 2020; Thomas et al., 2017). These novel indications rely on the ubiquitous presence of β-AR in tissues and organs as well as their important role in many physiological processes. Therefore, to better understand the complex role of β-AR, the development of novel molecular tools that enable their modulation with spatiotemporal precision is required. To that aim, in this work we present the first diffusible β-AR caged antagonist, which is only active on illumination with visible light. This molecule is based on the widely used beta blocker carvedilol, which has been highlighted as an interesting repurposing drug given its high affinity and special pharmacological profile (Kim et al., 2020). Here, we report the synthesis of caged-carvedilol (C-C) and its capacity to control the activity of β-AR using light. The activity of the developed molecule has been tested in a variety of physiological systems, from cells to freely behaving wildtype animals, demonstrating potential for a wide range of research applications.

RESULTS AND DISCUSSION

Design and synthesis

The molecular design of the caged antagonist first required the definition of the optimal emplacement for the photocleavable moiety. To assist this process, we performed computational studies depicting the binding mode of carvedilol in our target receptors (β-AR) (Figures 1A and S1). From these studies, the ethanolamine backbone was identified as the ideal area to introduce the caging moiety, considering that it has two reactive groups responsible for key binding interactions (Figures 1A and 1C) (Chan et al., 2016). A careful evaluation of the two possible caging positions highlighted the secondary amine as the best option, both for its increased reactivity and its location within the binding pocket. This amine is strongly interacting with key residues Asp121$^{3.32}$ and Asn329$^{7.39}$ (Warne et al., 2012), and has no space to allow for the introduction of a sterically demanding substituent. As a result, it was expected that the introduction of a cage in this position would induce repulsive interactions leading to a loss in affinity and functional activity (Figure 1B).
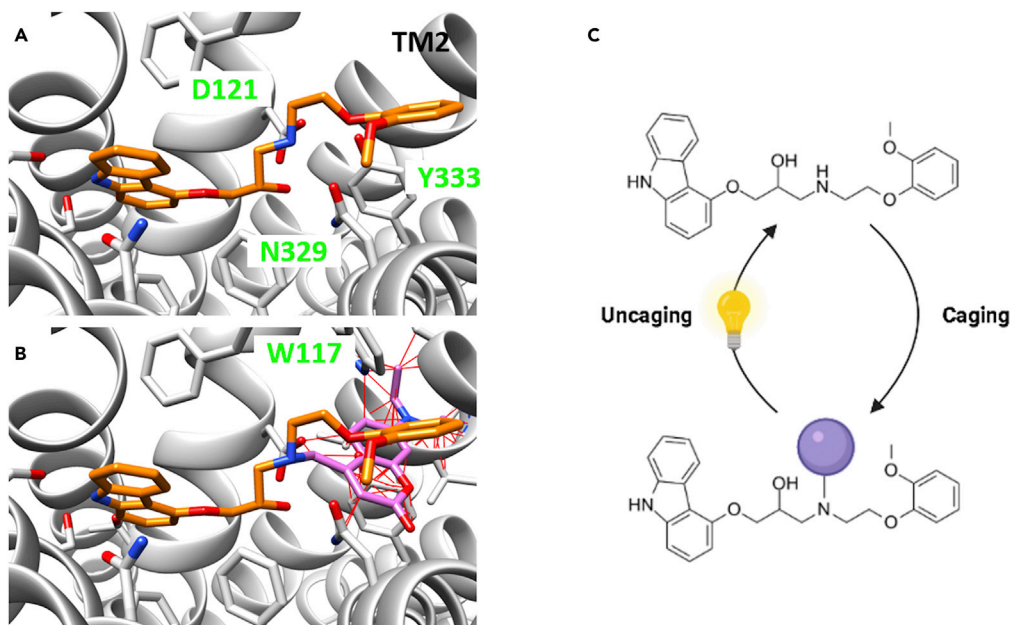
Figure 1. Design strategy of caged-carvedilol. Binding mode of carvedilol

(A and B) and placement of caged-carvedilol (B) in the crystal structure of β_1-AR (PDB id: 4AMJ) (Warne et al., 2012). Carvedilol is colored in orange, coumarinyl group is colored in pink, and red lines represent clashes with residues of the receptor.

(C) General strategy to produce an irreversible light-sensitive β-AR antagonist.

Following the determination of the caging position in carvedilol, the appropriate photocleavable moiety had to be selected. A variety of PPG have been developed in the last decades, where photochemical and physicochemical properties of the caging groups have been improved (Josa-Culleré and Llebaria, 2021). Nevertheless, o-nitrobenzyl and coumarin groups are the most classical PPG, very well characterized and extensively used in biological systems (Josa-Culleré and Llebaria, 2021; Klán et al., 2013; Ricart-Ortega et al., 2019). Among these options, [7-(diethylamino)coumarin-4-yl]methyl (DEACM) was chosen as a PPG because of its higher λ_{max}, which uncages within the visible range. Chemical synthesis of the caged beta blocker was achieved by direct N-alkylation of carvedilol with Br-DEACM in the presence of triethylamine (Scheme 1). This constitutes a rare approach to introduce the PPG, considering that protection of an amine group is usually achieved through a carbamate linker. However, the possible intramolecular reaction between the carbamate and the alcohol groups, prompted us to attempt the direct alkylation of the PPG to the secondary amine. On the other hand, Br-DEACM was synthesized through a described three-step synthesis (Scheme S1) (Goegan et al., 2018; Schönleber et al., 2002; Weinrich et al., 2017).
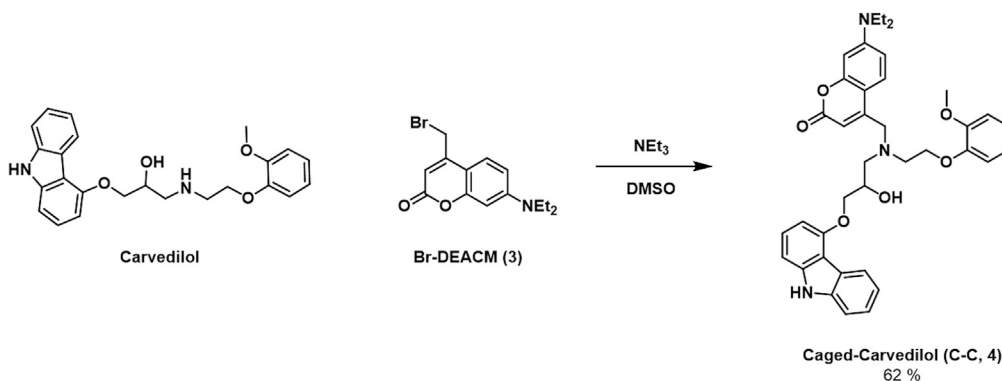
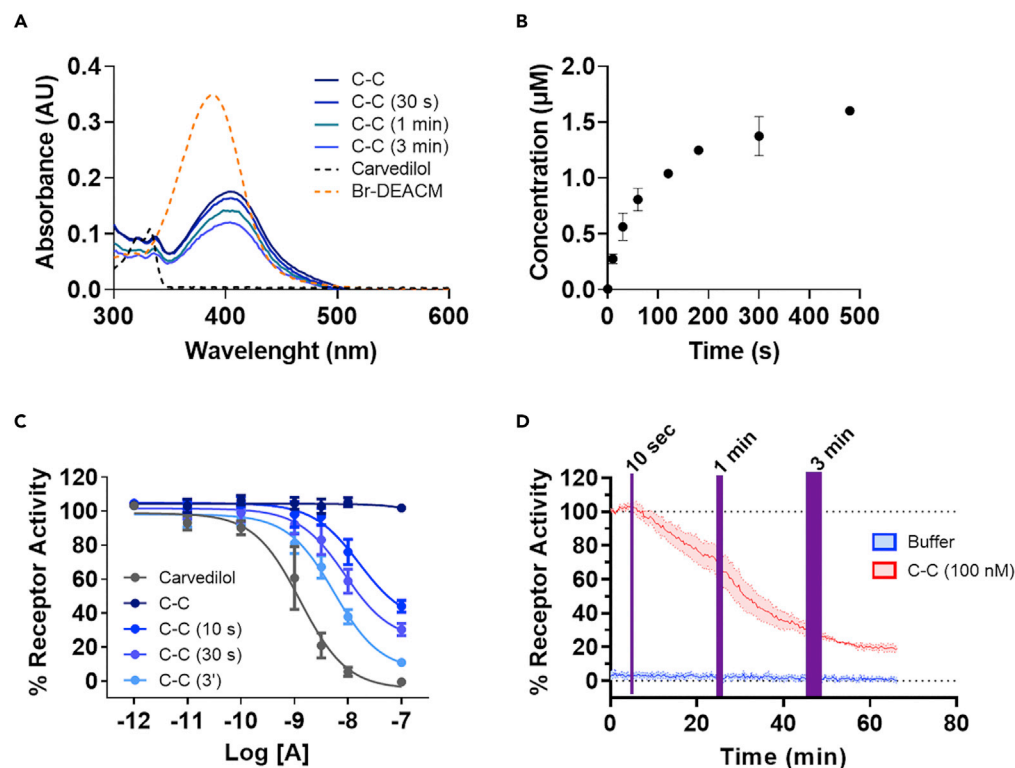**Scheme 1. Synthesis of caged-carvedilol (C-C)**

Figure 2. Photochemical and pharmacological characterization of caged-carvedilol

(A) UV-Vis spectra of 50 μM solutions of carvedilol, Br-DEACM and caged-carvedilol (C-C) in PBS (30% DMSO) before and after illumination with visible light (405 nm, 3 min).

(B) HPLC-MS quantification of released carvedilol after illumination of a 10 μM C-C aqueous sample (1% DMSO) for different times up to 9 min. Data are shown as the mean ± SEM of three independent experiments performed in duplicate.

(C) Dose-response curves of carvedilol and caged-carvedilol after different illumination times treated with a constant concentration of agonist cimaterol (3 nM). Data are shown as the mean ± SEM of three independent experiments performed in duplicate.

(D) Time course of intracellular cAMP dependent on the β-AR activity upon treatment with cimaterol (3 nM) alone (100% activity) or in combination with C-C (red line). Light pulses of different duration at 405 nm were directly applied to the cellular system (violet boxes). A HEK-293 cell line stably expressing the Epac-S^{H188} biosensor developed in our previous work (Duran-Corbera et al., 2020) was used for all pharmacological experiments. Data are shown as the mean ± SEM of three independent experiments performed in duplicate.

Photochemistry and *in vitro* photopharmacology

Firstly, UV-Vis spectroscopy experiments were performed to identify the optimal wavelength to trigger the uncaging. The absorbance spectrum of caged-carvedilol (Figure 2A) results from the combination of the main absorption peaks of its two components (carvedilol and Br-DEACM). The introduction of an *N*-coumarinyl group is responsible for the appearance of a new maximal absorption band between 395 and 410 nm. This transition, which is not present in the absorbance spectrum of carvedilol, can be used to induce the photolysis of the caging group. Illumination of C-C using 405 nm light resulted in a noticeable decrease in the absorption at λ$_{max}$, which illustrated the photocleavage of the coumarinyl group. In addition, stability of carvedilol to 405 nm light application was evaluated using HPLC and no degradation of the active beta blocker was detected (Figure S2).

Uncaging quantification was performed by HPLC-MS. These experiments evidenced that the proportion of carvedilol released from the developed compound is around 15% after 3 min of illumination at 405 nm (Figure 2B). Longer illumination times did not result in higher uncaging but in compound degradation (Figure S3). For this reason, 3 min was set as the maximum illumination time for subsequent pharmacological experiments. It is worth mentioning that the decrease of C-C was larger than 15% after 3 min illumination,

indicating that there are other products of degradation. Although these undetermined products may possess biological activities, the pharmacological results obtained in this study are compatible with the release of carvedilol. Further developments of the molecule may address this topic by modifying the position of the PPG or its linker. Indeed, the slower photolytic reaction observed in comparison to other caged molecules can be attributed to the linkage of the PPG through direct alkylation, which renders a relatively stable photocage. Indeed, it is known that carbamate linkers of amino groups facilitate the deprotection reaction and enable fast and efficient photocleavage (Slanina et al., 2017). However, for our purposes, working with a compound with lower photolytic reactivity facilitates purification and handling in biological assays, thus allowing for a precise administration of highly potent molecules, such as carvedilol which counts with sub nanomolar binding affinities for β-AR.

Once the photochemical properties of the developed compound were characterized, *in vitro* experiments were performed to assess its potential to irreversibly control the activity of β-AR with light. These experiments were performed using a recently described cellular system, which endogenously expresses β_2-AR and is stably transfected with a cAMP Epac biosensor (Duran-Corbera et al., 2020; Klarenbeek et al., 2015). Light-dependent release of carvedilol was examined by antagonizing the activating effect of the β-AR agonist cimaterol. Results showed that the introduction of the caging moiety to carvedilol completely abolished its functional activity at the concentrations tested. In addition, the application of light to the C-C triggered the antagonist activity over the cimaterol receptor activation. For instance, 100 nM samples subjected to 10 s illumination already reduced the activation state of β_2-AR by 55%. Longer illuminations resulted in higher inhibition of the system, with 90% of receptor function inhibition achieved with 100 nM caged-carvedilol illuminated for 3 min at 405 nm (Figures 2C and 2D). Therefore, these results mark the potential of the developed compound to regulate the activation state of β-AR with temporal precision using light.

Light-control of cardiac function by caged-carvedilol

Carvedilol is a non-selective beta blocker, highly used for the treatment of a diverse number of cardiac conditions. For this reason, the light-triggered effects of caged-carvedilol on the cardiac function were assessed. First, isolated perfused mice hearts were used (Figures 3A, 3C and S4). This *ex vivo* technique constitutes a good physiological model to evaluate the light-dependent modulation of the cardiac frequency exerted by the caged beta blocker (Bell et al., 2011).

Control hearts were treated with isoprenaline (100 nM, for 10 min) which induced a significant increase in heart rate (Figure 3A). A peak of about 160% of baseline values was observed after 3-4 min of starting the agonist perfusion. This increment in the cardiac frequency was maintained for the entire duration of isoprenaline infusion. A progressive decline in the measurements was only observed after washing the agonist out. The increase in heart rate induced by isoprenaline was not modified when the perfused hearts were simultaneously treated with 25 μM of C-C. In contrast, when the same experiment was performed with 25 μM of illuminated C-C the increment in the cardiac frequency was not observed (Figures 3A and 3C). This indicated that on light application free carvedilol had been released and was consequently blocking the effects of isoprenaline in perfused hearts.

To extrapolate the promising results obtained *ex vivo*, the potential of the developed compound as a light-sensitive beta blocker was also evaluated in an *in vivo* model. Zebrafish larvae of 7 days after fertilization (dpf) were used for this purpose considering that the subjects are transparent, which enabled non-invasive heart monitorization. Exposures to the different treatment conditions were conducted for 1 h and the cardiac rhythm of the larvae was monitored using a microscope equipped with a camera (Video S1). The obtained results were in good agreement with the cardiac effects observed in mice perfused hearts (Figures 3A and 3C). No significant effects were measured on heart rate of animals treated with 25 μM C-C. In contrast, subjects exposed to the caged compound illuminated for only 30 s already presented a significantly reduced cardiac rhythm; furthermore, larvae illuminated for 3 min reduced the heart rate by 40%. A comparable effect was observed when larvae were treated with 10 μM carvedilol, corroborating that the cardiac effects observed after illumination are related to the photolytic release of the beta blocker (Figure 3B). This activity is readily observable by visual inspection (Video S1) and when plotting the heartbeat (Figure 3D). Indeed, a delay in frequency becomes evident on the addition of illuminated caged-carvedilol in comparison to control animals, similar to what it is observed in perfused mice hearts (Figure 3C). Therefore, we have successfully developed a compound that enables a selective control of cardiac function through the application of light in two distinct physiological models.
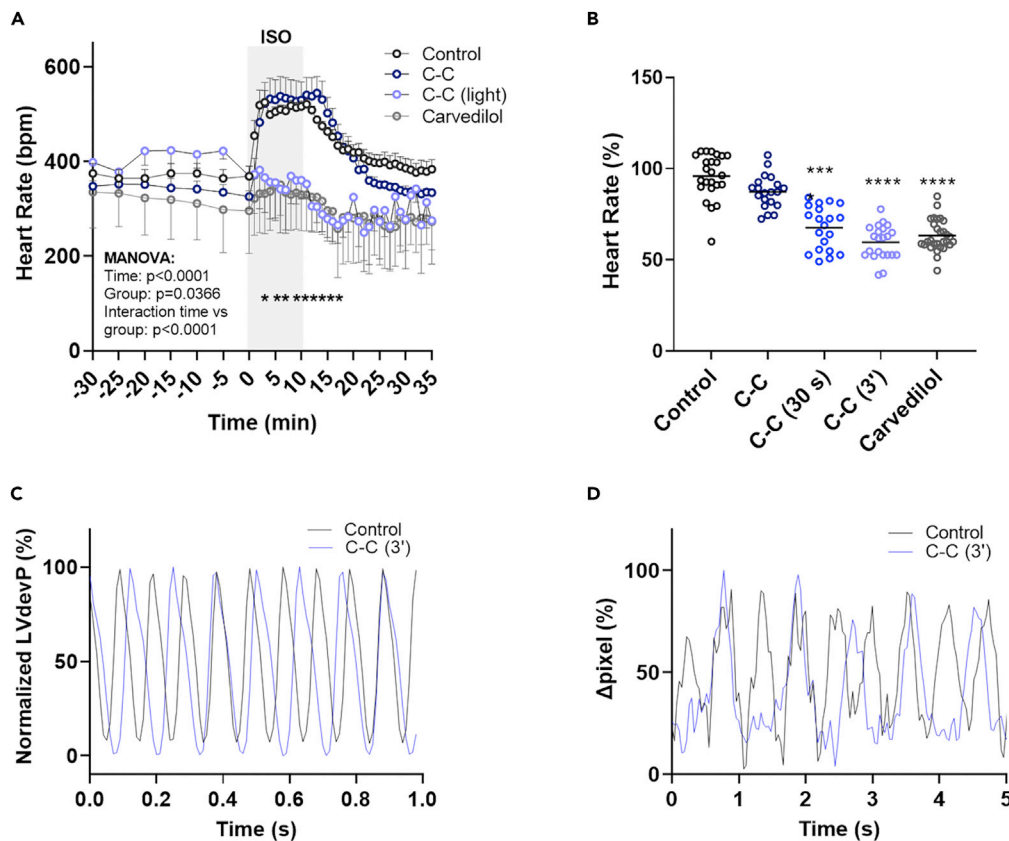
Figure 3. Evaluation of the light-dependent cardiac effects of C-C in two physiological models

(A) Heart rate monitorization in isolated mice hearts treated with 100 nM isoprenaline in the absence or presence of 25 μM carvedilol caged or uncaged (after 2 × 2.5 min illumination at 405 nm) and 100 nM carvedilol (n = 3-5). Data are shown as the mean ± SEM Statistical differences were assessed by repeated measures ANOVA(MANOVA) and Tukey's post hoc test.

(B) Normalized heart rate of zebrafish larvae treated with 1% DMSO (control), 10 μM carvedilol, 25 μM caged-carvedilol in the dark (C-C) and after 30 s (C-C (30s)) and 3 min (C-C (3')) illuminations at 405 nm (n = 20-29). Data are shown as scattered plots, where each point represents a biological replicate and the black line represents the mean value. Statistical differences were assessed by performing a one-way ANOVA followed by Tukey's multiple comparisons test. Significant differences are denoted for adjusted p values as follows: ***p < 0.001 and ****p < 0.0001.

(C) Normalized left ventricular developed pressure (LvdevP) of mice perfused hearts treated with isoprenaline and isoprenaline +25 μM C-C illuminated.

(D) Normalized cardiac contractions of control zebrafish larvae and larvae exposed to 25 μM C-C illuminated. Cardiac contractions were monitored as pixel variation in the recorded videos.

Cardiac modulation with the application of light was firstly achieved by means of optogenetics (Bruegmann et al., 2016; Crocini et al., 2017; Koopman et al., 2017; Quinn et al., 2016; Wang et al., 2017). The use of this innovative technique provided a valuable tool for the investigation of cardiac physiology and pointed to possible therapeutic applications based on the precise control of the heart rhythm using light. However, this approach requires genetic manipulation, which limits its clinical prospects. More recently, light-dependent cardiac modulation of rats and frog tadpoles was reported using a photoswitchable agonist targeting muscarinic receptors (Riefolo et al., 2019). However, photocardiac control through the modulation of the adrenergic pathway had never been reported. Therefore, the developed caged-carvedilol enlarges the photopharmacological toolbox to study the complex mechanisms of cardiac function. In addition, the proof of concept of this study, in which a photolytic release of an approved drug is demonstrated, highlights the potential of this approach for future therapeutic applications.

In vivo modulation of animal behavior

Finally, it is well described that the activation of β-AR is related to the "fight or flight" response (Man et al., 2020). A recent study reports that blocking the β-adrenergic signaling pathway significantly reduces the
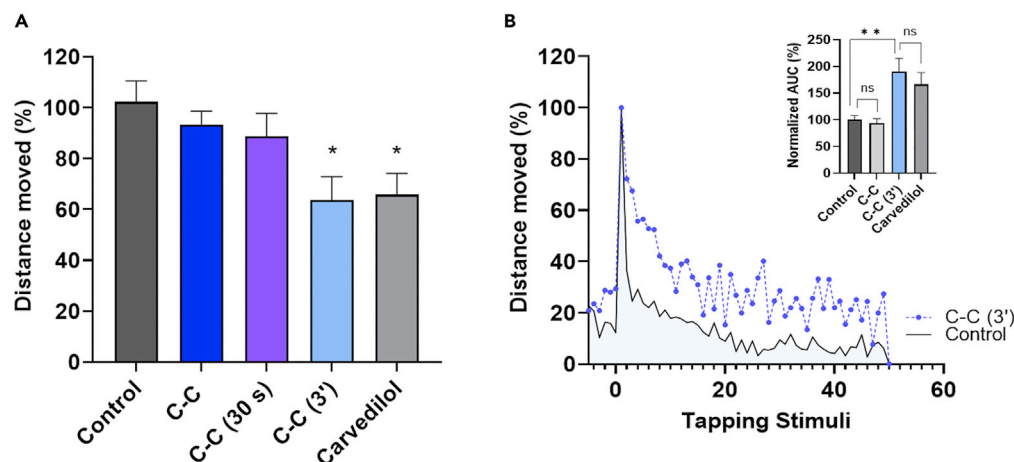
Figure 4. Zebrafish larvae escape response and their habituation behavior

(A) Normalized distance moved (mean $\pm$ SEM) during the startle response of the zebrafish larvae (7 dpf) treated with 1% DMSO, 10 μM carvedilol and 25 μM C-C, either in the dark or after 30 s and 3 min illuminations (405 nm); startle response was measured immediately after the application of the first tapping stimulus (n = 26-44). Statistical differences were assessed by performing a one-way ANOVA followed by Tukey's multiple comparisons test. Significant differences between the analyzed groups are denoted for adjusted p values as follows: *p < 0.05.

(B) Habituation profile of zebrafish larvae treated with 1% DMSO or 25 μM C-C illuminated for 3 min (405 nm). The profile is represented as the decrease in the normalized distance moved by the animals across 50 tapping stimuli delivered with 1 s intervals. AUCs (mean $\pm$ SEM) of the two groups and of 10 μM carvedilol and 25 μM C-C in the dark are represented as an inset to the plot (n = 21-46). Statistical differences were assessed by performing a one-way ANOVA followed by Tukey's multiple comparisons test. Significant differences between the analyzed groups are denoted for adjusted p values as follows: **p < 0.01.

escape response of zebrafish embryos to external visual stimuli (Gauthier and Vijayan, 2019). Similarly, we evaluated here the modulation of the vibrational-evoked startle response exerted by the developed caged compound under different illumination conditions using zebrafish larvae. In these experiments, the animals were exposed to different treatments (carvedilol, C-C and C-C illuminated for 30 s and 3 min) during 1 h under dark conditions. Following the exposure, animals were left to acclimatize for 10 min and then the monitorization of zebrafish behavior was conducted. Initially, following the acclimatization period, the basal locomotor activity (BLA) of the different groups of zebrafish was recorded. Then, the studied groups were subjected to 50 consecutive vibrational stimuli which assessed two behavioral parameters, vibrational-evoked startle response and its habituation after repetitive stimuli (Faria et al., 2019).

Results showed no significant differences in BLA between the treatment groups, suggesting that blocking the adrenergic pathway does not have effects on the mobility of zebrafish larvae (Figure S5). On the other hand, a significant reduction of the startle response to the first tapping stimulus was observed only when larvae were exposed to carvedilol or C-C illuminated for 3 min. Both treatments reduced the escape response of the zebrafish larvae similarly, by approximately 35% (Figure 4A). This, according to the reported literature, indicated that in both zebrafish groups the adrenergic drive had been blocked (Gauthier and Vijayan, 2019). In addition, habituation of the vibrational-evoked escape response was significantly delayed (AUC above the control) by carvedilol and C-C illuminated for 3 min (Figures 4B and S5). These results demonstrate that groups treated with carvedilol have an altered non-associative learning process, as the larvae maintained a higher escape response through the 50 consecutive vibrational stimuli. Therefore, we have successfully achieved a light-dependent control of zebrafish behavior using the developed caged beta blocker.

The complex mechanisms underlying the effects observed on stimuli habituation are not completely understood and can be a consequence of multiple factors as numerous receptors and neural circuits can be involved in this process (Best et al., 2008; Randlett et al., 2019). For instance, it has been described that modulation of the cholinergic and serotonergic pathways can affect this simple form of non-associative learning (Best et al., 2008). Of interest, interactions of carvedilol with the muscarinic receptor M2 and the serotonin receptor 5-HT$_{2A}$ have been reported in the literature (Murnane et al., 2019; Xu et al., 2006). In addition, other aminergic systems, such as dopamine D2 receptors have also been involved in

behavioral plasticity and habituation (Randlett et al., 2019). Of interest, D2 and β1-AR have been found to co-localize in prefrontal cortical cells affecting each other functional properties on activation (Montezinho et al., 2006). Overall, the significant effects of carvedilol and uncaged C-C observed in the habituation behavior of zebrafish larvae could be because of the modulation of these or other pathways. However, given the wide distribution of β-AR in the nervous system (Reznikoff et al., 1986) it can be difficult to map the neural circuits involved. In this context, caged-carvedilol could represent an interesting research tool to explore the involvement of β-AR in this and other animal behaviors, thus providing a better understanding on their important role in the central nervous system.

In this work we report the first diffusible caged antagonist targeting adrenoceptors active in native tissues and in live animals. This new molecule complements the photopharmacological toolbox based on caged compounds targeting β-AR, which was until now composed of agonists (Vaniotis et al., 2013) and surface-attached antagonists (Mu et al., 2018). Carvedilol, a non-selective beta blocker, was synthetically modified through alkylation of the secondary amine with a coumarin caging group. Photolysis of C-C occurred within the visible range (405 nm) which is ideal to avoid UV phototoxicity in physiological systems. Light-dependent effects of C-C were assessed in different biological systems, in both *in vitro* and *in vivo* settings. Caged-carvedilol showed no biological activity in the assayed systems. Only on light application, free carvedilol was released and the biological effects, which were similar to the groups treated with the control beta blocker, were observed. In *in vitro* experiments, increasing inhibition of β-AR were directly correlated with increasing illumination times of the caged compound. Light-triggered effect on heart rate was comparable in two distinct models: Langendorff-perfused mice hearts and living zebrafish larvae. In both systems the cardiac frequency was only modulated on illumination of C-C. Finally, the effects of the compound on zebrafish behavior were also assayed to evaluate the physiological effects of β-AR in the nervous system. Uncaged C-C showed a significant reduction of the zebrafish escape response to an acoustic/vibrational stimulus. In addition, the habituation process to a series of repetitive stimuli was noticeably delayed in experimental groups treated with illuminated C-C. The successful application of the caged beta blocker in a range of physiological systems highlights this molecule as a valuable research tool to deepen the current knowledge on adrenoceptor function and signaling. In addition, this work opens up new avenues for the development of light-regulated drugs, which because of their localized release can be more efficient and show reduced side effects in future therapeutic applications.

Limitations of the study

Although we show that the activity of β-AR can be successfully controlled with temporal precision using C-C and light (Figure 2D), technical limitations in the illumination system did not allow us to demonstrate a localized release of carvedilol in a biological system. We hope that future projects involving the molecular tool presented here will help tackling this challenge to get answers with physiological relevance. One of these questions could be the role of adrenoceptors in the short-term habituation, which is a primitive form of implicit learning. When an animal is exposed to repeated stimuli, it responds to the first few ones but, if the stimulus is neither beneficial nor harmful, the animal learns to ignore it (Kandel, 1991). In this study we have analyzed the short-term habituation of the startle response evoked by acoustic/vibrational stimuli, which occurs when zebrafish larvae are exposed to repeated stimulation at short interstimulus intervals. We show that habituation is altered on release of carvedilol but the exact mechanism and the nervous system region involved have not been explored. Finally, a common issue when developing cage compounds that it is mentioned in the main text is the generation of products of degradation after uncaging, including the caging moiety (DEACM in the present work). Although these products are unlikely to affect the specific process under study, they may possess other biological activities.

STAR★METHODS

Detailed methods are provided in the online version of this paper and include the following:

- KEY RESOURCES TABLE
- RESOURCE AVAILABILITY
  - Lead contact
  - Materials availability
  - Data and code availability
- EXPERIMENTAL MODEL AND SUBJECT DETAILS
  - Cell lines

- ○ Mice for *ex vivo* assays
- ○ Zebrafish larvae for *in vivo* assays
- ● METHOD DETAILS
  - ○ Synthesis and compound characterization
  - ○ Molecular modeling
  - ○ Photochemistry
  - ○ Cell culture and transfection
  - ○ Pharmacology
  - ○ Langendorff heart experiments
  - ○ Assays in zebrafish larvae
- ● QUANTIFICATION AND STATISTICAL ANALYSIS

SUPPLEMENTAL INFORMATION

Supplemental information can be found online at https://doi.org/10.1016/j.isci.2022.105128.

DECLARATION OF INTERESTS

The authors declare no competing interests.

REFERENCES

Agnetta, L., Kauk, M., Canizal, M.C.A., Messerer, R., Holzgrabe, U., Hoffmann, C., and Decker, M. (2017). A photoswitchable dualsteric ligand controlling receptor efficacy. Angew. Chem. Int. Ed. *56*, 7282–7287. https://doi.org/10.1002/anie.201701524.

Altosaar, K., Balaji, P., Bond, R.A., Bylund, D.B., Cotecchia, S., Devost, D., Doze, V.A., Eikenburg,

D.C., Gora, S., Goupil, E., et al. (2019). Adrenoceptors (version 2019.4) in the IUPHAR/BPS Guide to Pharmacology Database (IUPHAR/BPS Guide to Pharmacology CITE). http://journals.ed.ac.uk/gtopdb-cite/article/view/3158.

Bahamonde, M.I., Taura, J., Paoletta, S., Gakh, A.A., Chakraborty, S., Hernando, J., Fernández-Dueñas, V., Jacobson, K.A., Gorostiza, P., and

Ciruela, F. (2014). Photomodulation of G Protein-Coupled adenosine receptors by anovel light-switchable ligand. Bioconjug. Chem. *25*, 1847–1854. https://doi.org/10.1021/bc5003373.

Baker, J.G. (2005). The selectivity of β-adrenoceptor antagonists at the human β 1, β 2 and β 3 adrenoceptors. Br. J. Pharmacol. *144*, 317–322. https://doi.org/10.1038/sj.bjp.0706048.

Banghart, M.R., He, X.J., and Sabatini, B.L. (2018). A caged enkephalin optimized for simultaneously probing mu and delta opioid receptors. ACS Chem. Neurosci. *9*, 684–690. https://doi.org/10.1021/acschemneuro.7b00485.

Banghart, M.R., and Sabatini, B.L. (2012). Photoactivatable neuropeptides for spatiotemporally precise delivery of opioids in neural tissue. Neuron *73*, 249–259. https://doi.org/10.1016/j.neuron.2011.11.016.

Banghart, M.R., Williams, J.T., Shah, R.C., Lavis, L.D., and Sabatini, B.L. (2013). Caged naloxone reveals opioid signaling deactivation kinetics. Mol. Pharmacol. *84*, 687–695. https://doi.org/10.1124/mol.113.088096.

Bell, R.M., Mocanu, M.M., and Yellon, D.M. (2011). Retrograde heart perfusion: the Langendorff technique of isolated heart perfusion. J. Mol. Cell. Cardiol. *50*, 940–950. https://doi.org/10.1016/j.yjmcc.2011.02.018.

Best, J.D., Berghmans, S., Hunt, J.J.F.G., Clarke, S.C., Fleming, A., Goldsmith, P., and Roach, A.G. (2008). Non-associative learning in larval zebrafish. Neuropsychopharmacology *33*, 1206–1215. https://doi.org/10.1038/sj.npp.1301489.

Broichhagen, J., Frank, J.A., and Trauner, D. (2015). A roadmap to success in photopharmacology. Acc. Chem. Res. *48*, 1947–1960. https://doi.org/10.1021/acs.accounts.5b00129.

Bruegmann, T., Boyle, P.M., Vogt, C.C., Karathanos, T.v., Arevalo, H.J., Fleischmann, B.K., Trayanova, N.A., and Sasse, P. (2016). Optogenetic defibrillation terminates ventricular arrhythmia in mouse hearts and human simulations. J. Clin. Invest. *126*, 3894–3904. https://doi.org/10.1172/JCI88950.

Callaway, E.M., and Katz, L.C. (1993). Photostimulation using caged glutamate reveals functional circuitry in living brain slices. Proc. Natl. Acad. Sci. USA *90*, 7661–7665. https://doi.org/10.1073/pnas.90.16.7661.

Chan, H.C.S., Filipek, S., and Yuan, S. (2016). The principles of ligand specificity on beta-2-adrenergic receptor. Sci. Rep. *6*, 34736. https://doi.org/10.1038/srep34736.

Crocini, C., Ferrantini, C., Pavone, F.S., and Sacconi, L. (2017). Optogenetics gets to the heart: a guiding light beyond defibrillation. Prog.Biophys. Mol. Biol. *130*, 132–139. https://doi.org/10.1016/j.pbiomolbio.2017.05.002.

Donthamsetti, P.C., Winter, N., Schönberger, M., Levitz, J., Stanley, C., Javitch, J.A., Isacoff, E.Y., and Trauner, D. (2017). Optical control of dopamine receptors using a photoswitchable tethered inverse agonist. J. Am. Chem. Soc. *139*, 18522–18535. https://doi.org/10.1021/jacs.7b07659.

Duran-Corbera, A., Catena, J., Otero-Viñas, M., Llebaria, A., and Rovira, X. (2020). Photoswitchable antagonists for a precise spatiotemporal control of β₂-adrenoceptors. J. Med. Chem. *63*, 8458–8470. https://doi.org/10.1021/acs.jmedchem.0c00831.

Duran-Corbera, A., Faria, M., Ma, Y., Prats, E., Dias, A., Catena, J., Martinez, K.L., Raldua, D., Llebaria, A., and Rovira, X. (2022). A

photoswitchable ligand targeting the β₁-adrenoceptor enables light-control of the cardiac rhythm**. Angew.Chem. Int. Ed. https://doi.org/10.1002/anie.202203449.

Ellis-Davies, G.C.R. (2020). Useful caged compounds for cell physiology. Acc. Chem. Res. *53*, 1593–1604. https://doi.org/10.1021/acs.accounts.0c00292.

Ellis-Davies, G.C.R. (2007). Caged compounds: photorelease technology for control of cellular chemistry and physiology. Nat. Methods *4*, 619–628. https://doi.org/10.1038/nmeth1072.

Faria, M., Garcia-Reyero, N., Padrós, F., Babin, P.J., Sebastián, D., Cachot, J., Prats, E., Arick, M., Rial, E., Knoll-Gellida, A., et al. (2015). Zebrafish models for human acute organophosphorus poisoning. Sci. Rep. *5*, 15591. https://doi.org/10.1038/srep15591.

Faria, M., Prats, E., Novoa-Luna, K.A., Bedrossiantz, J., Gómez-Canela, C., Gómez-Olíván, L.M., and Raldúa, D. (2019). Development of a vibrational startle response assay for screening environmental pollutants and drugs impairing predator avoidance. Sci. Total Environ. *650*, 87–96. https://doi.org/10.1016/j.scitotenv.2018.08.421.

Faria, M., Wu, X., Luja-Mondragón, M., Prats, E., Gómez-Olíván, L.M., Piña, B., and Raldúa, D. (2020). Screening anti-predator behaviour in fish larvae exposed to environmental pollutants. Sci. Total Environ. *714*, 136759. https://doi.org/10.1016/j.scitotenv.2020.136759.

Filoni, A., Ambrogio, F., de Marco, A., Pacifico, A., and Bonamonte, D. (2021). Topical beta-blockers in dermatologic therapy. Dermatol.Ther. *34*. https://doi.org/10.1111/dth.15016.

Font, J., López-Cano, M., Notartomaso, S., Scarselli, P., di Pietro, P., Bresolí-Obach, R., Battaglia, G., Malhaire, F., Rovira, X., Catena, J., et al. (2017). Optical control of pain in vivo with a photoactive mGlu5 receptor negative allosteric modulator. Elife *6*. https://doi.org/10.7554/eLife.23545.

Frank, J.A., Yushchenko, D.A., Fine, N.H.F., Duca, M., Citir, M., Broichhagen, J., Hodson, D.J., Schultz, C., and Trauner, D. (2017). Optical control of GPR40 signalling in pancreatic β-cells. Chem. Sci. *8*, 7604–7610. https://doi.org/10.1039/C7SC01475A.

Fuchter, M.J. (2020). On the promise of photopharmacology using photoswitches: amedicinal chemist's perspective. J. Med. Chem. *63*, 11436–11447. https://doi.org/10.1021/acs.jmedchem.0c00629.

Gauthier, P.T., and Vijayan, M.M. (2019). A rapid zebrafish embryo behavioral biosensor that is capable of detecting environmental β-blockers. Environ. Pollut. *250*, 493–502. https://doi.org/10.1016/j.envpol.2019.03.053.

Gelosa, P., Castiglioni, L., Camera, M., and Sironi, L. (2020). Repurposing of drugs approved for cardiovascular diseases: opportunity or mirage? Biochem. Pharmacol. *177*, 113895. https://doi.org/10.1016/j.bcp.2020.113895.

Goegan, B., Terzi, F., Bolze, F., Cambridge, S., and Specht, A. (2018). Synthesis and characterization of photoactivatable doxycycline

analogues bearing two-photon-sensitive photoremovable groups suitable for light-induced gene expression. Chembiochem *19*, 1341–1348. https://doi.org/10.1002/cbic.201700628.

Gómez-Santacana, X., de Munnik, S.M., Vijayachandran, P., Da Costa Pereira, D., Bebelman, J.P.M., de Esch, I.J.P., Vischer, H.F., Wijtmans, M., and Leurs, R. (2018). Photoswitching the efficacy of a small-molecule ligand for a peptidergic GPCR: from antagonism to agonism. Angew. Chem. Int. Ed. *57*, 11608–11612. https://doi.org/10.1002/anie.201804875.

Hauwert, N.J., Mocking, T.A.M., da Costa Pereira, D., Kooistra, A.J., Wijnen, L.M., Vreeker, G.C.M., Verweij, E.W.E., de Boer, A.H., Smit, M.J., de Graaf, C., et al. (2018). Synthesis and characterization of a bidirectional photoswitchable antagonist toolbox for real-time GPCR photopharmacology. J. Am. Chem. Soc. *140*, 4232–4243. https://doi.org/10.1021/jacs.7b11422.

Hüll, K., Fernández-Dueñas, V., Schönberger, M., López-Cano, M., Trauner, D., and Ciruela, F. (2021). Optical control of adenosine-mediated pain modulation. Bioconjug. Chem. *32*, 1979–1983. https://doi.org/10.1021/acs.bioconjchem.1c00387.

Hüll, K., Morstein, J., and Trauner, D. (2018). *In vivo* photopharmacology. Chem. Rev. *118*, 10710–10747. https://doi.org/10.1021/acs.chemrev.8b00037.

Ishchenko, A., Stauch, B., Han, G.W., Batyuk, A., Shiriaeva, A., Li, C., Zatsepin, N., Weierstall, U., Liu, W., Nango, E., et al. (2019). Toward G protein-coupled receptor structure-based drug design using X-ray lasers. IUCrJ *6*, 1106–1119. https://doi.org/10.1107/S2052252519013137.

Josa-Culleré, L., and Llebaria, A. (2021). In the search for photocages cleavable with visible light: an overview of recent advances and chemical strategies. ChemPhotoChem *5*, 296–314. https://doi.org/10.1002/cptc.202000253.

Kandel, E.R. (1991). Cellular mechanisms of learning and the biological Basis of Individuality. In Principles of Neural Science (Elsevier), pp. 1009–1031.

Kim, J., Grotegut, C.A., Wisler, J.W., Mao, L., Rosenberg, P.B., Rockman, H.A., and Lefkowitz, R.J. (2020). The β-arrestin-biased β-adrenergic receptor blocker carvedilol enhances skeletal muscle contractility. Proc. Natl. Acad. Sci. USA *117*, 12435–12443. https://doi.org/10.1073/pnas.1920310117.

Klán, P., Šolomek, T., Bochet, C.G., Blanc, A., Givens, R., Rubina, M., Popik, V., Kostikov, A., and Wirz, J. (2013). Photoremovable protecting groups in chemistry and biology: reaction mechanisms and efficacy. Chem. Rev. *113*, 119–191. https://doi.org/10.1021/cr300177k.

Klarenbeek, J., Goedhart, J., van Batenburg, A., Groenewald, D., and Jalink, K. (2015). Fourth-generation epac-based fret sensors for camp feature exceptional brightness, photostability and dynamic range: characterization of dedicated sensors for flim, for ratiometry and with high affinity. PLoS One *10*, e0122513. https://doi.org/10.1371/journal.pone.0122513.

Koopman, C.D., Zimmermann, W.H., Knöpfel, T., and de Boer, T.P. (2017). Cardiac optogenetics: using light to monitor cardiac physiology. Basic Res. Cardiol. *112*, 56. https://doi.org/10.1007/s00395-017-0645-y.

Koshimizu, T. (2004). Carvedilol selectively inhibits oscillatory intracellular calcium changes evoked by human ?1D- and ?1B-adrenergic receptors. Cardiovasc.Res. *63*, 662–672. https://doi.org/10.1016/j.cardiores.2004.05.014.

Lerch, M.M., Hansen, M.J., van Dam, G.M., Szymanski, W., and Feringa, B.L. (2016). Emerging targets in photopharmacology. Angew. Chem. Int. Ed. *55*, 10978–10999. https://doi.org/10.1002/anie.201601931.

López-Cano, M., Font, J., Aso, E., Sahlholm, K., Cabré, G., Giraldo, J., de Koninck, Y., Hernando, J., Llebaria, A., Fernández-Dueñas, V., and Ciruela, F. (2021). Remote local photoactivation of morphine produces analgesia without opioid-related adverse effects. Br. J. Pharmacol. https://doi.org/10.1111/bph.15645.

Man, K.N.M., Bartels, P., Horne, M.C., and Hell, J.W. (2020). Tissue-specific adrenergic regulation of the L-type Ca $^{2+}$ Channel Ca $_V$ 1.2. Sci. Signal. *13*. https://doi.org/10.1126/scisignal.abc6438.

Montezinho, L.P., Castro, M.M.C.A., Duarte, C.B., Penschuck, S., Geraldes, C.F.G.C., and Mørk, A. (2006). The interaction between dopamine D $_2$ -like and beta-adrenergic receptors in the prefrontal cortex is altered by mood-stabilizing agents. J. Neurochem. *96*, 1336–1348. https://doi.org/10.1111/j.1471-4159.2005.03654.x.

Morstein, J., Dacheux, M.A., Norman, D.D., Shemet, A., Donthamsetti, P.C., Citir, M., Frank, J.A., Schultz, C., Isacoff, E.Y., Parrill, A.L., et al. (2020). Optical control of lysophosphatidic acid signaling. J. Am. Chem. Soc. *142*, 10612–10616. https://doi.org/10.1021/jacs.0c02154.

Mu, C., Shi, M., Liu, P., Chen, L., and Marriott, G. (2018). Daylight-mediated, passive, and sustained release of the glaucoma drug timolol from a contact lens. ACS Cent. Sci. *4*, 1677–1687. https://doi.org/10.1021/acscentsci.8b00641.

Muralidharan, S., and Nerbonne, J.M. (1995). Photolabile "caged" adrenergic receptor agonists and related model compounds. J. Photochem. Photobiol., B *27*, 123–137. https://doi.org/10.1016/1011-1344(94)07063-T.

Murnane, K.S., Guner, O.F., Bowen, J.P., Rambacher, K.M., Moniri, N.H., Murphy, T.J., Daphney, C.M., Oppong-Damoah, A., and Rice, K.C. (2019). The adrenergic receptor antagonist carvedilol interacts with serotonin 2A receptors both in vitro and in vivo. Pharmacol. Biochem.Behav. *181*, 37–45. https://doi.org/10.1016/j.pbb.2019.04.003.

Peixoto, R., Pereira, M. de L., and Oliveira, M. (2020). Beta-blockers and cancer: where are we? Pharmaceuticals *13*, 105. https://doi.org/10.3390/ph13060105.

Perez, M Dianne (2005). The Adrenergic Receptors in the 21st Century (Humana Press).

Quinn, T.A., Camelliti, P., Rog-Zielinska, E.A., Siedlecka, U., Poggioli, T., O'Toole, E.T., Knöpfel, T., and Kohl, P. (2016). Electrotonic coupling of excitable and nonexcitable cells in the heart

revealed by optogenetics. Proc. Natl. Acad. Sci. USA *113*, 14852–14857. https://doi.org/10.1073/pnas.1611184114.

Randlett, O., Haesemeyer, M., Forkin, G., Shoenhard, H., Schier, A.F., Engert, F., and Granato, M. (2019). Distributed plasticity drives visual habituation learning in larval zebrafish. Curr.Biol. *29*, 1337–1345.e4. https://doi.org/10.1016/j.cub.2019.02.039.

Reznikoff, G.A., Manaker, S., Rhodes, C.H., Winokur, A., and Rainbow, T.C. (1986). Localization and quantification of beta-adrenergic receptors in human brain. Neurology *36*, 1067. https://doi.org/10.1212/wnl.36.8.1067.

Ricart-Ortega, M., Font, J., and Llebaria, A. (2019). GPCR photopharmacology. Mol. Cell. Endocrinol. *488*, 36–51. https://doi.org/10.1016/j.mce.2019.03.003.

Riefolo, F., Matera, C., Garrido-Charles, A., Gomila, A.M.J., Sortino, R., Agnetta, L., Claro, E., Masgrau, R., Holzgrabe, U., Batlle, M., et al. (2019). Optical control of cardiac function with a photoswitchable muscarinic agonist. J. Am. Chem. Soc. *141*, 7628–7636. https://doi.org/10.1021/jacs.9b03505.

Schönberger, M., and Trauner, D. (2014). A photochromic agonist for μ-opioid receptors. Angew. Chem. Int. Ed. *53*, 3264–3267. https://doi.org/10.1002/anie.201309633.

Schönleber, R.O., Bendig, J., Hagen, V., and Giese, B. (2002). Rapid photolytic release of cytidine 5′-diphosphate from a coumarin derivative: a new tool for the investigation of ribonucleotide reductases. Bioorg. Med. Chem. *10*, 97–101. https://doi.org/10.1016/S0968-0896(01)00254-1.

Slanina, T., Shrestha, P., Palao, E., Kand, D., Peterson, J.A., Dutton, A.S., Rubinstein, N., Weinstain, R., Winter, A.H., and Klán, P. (2017). In search of the perfect photocage: structure–reactivity relationships in *meso* -methyl BODIPY photoremovable protecting groups. J. Am. Chem. Soc. *139*, 15168–15175. https://doi.org/10.1021/jacs.7b08532.

Stapleton, M.P. (1997). Sir James Black and propranolol.The role of the basic sciences in the history of cardiovascular pharmacology. Tex. Heart Inst. J. *24*, 336–342.

Tapia, L., Alfonso, I., and Solà, J. (2021). Molecular cages for biological applications. Org. Biomol. Chem. *19*, 9527–9540. https://doi.org/10.1039/D1OB01737C.

Taura, J., Nolen, E.G., Cabré, G., Hernando, J., Squarcialupi, L., López-Cano, M., Jacobson, K.A., Fernández-Dueñas, V., and Ciruela, F. (2018). Remote control of movement disorders using a photoactive adenosine A2A receptor antagonist. J. Contr. Release *283*, 135–142. https://doi.org/10.1016/j.jconrel.2018.05.033.

Thomas, B., Kurien, J.S., Jose, T., Ulahannan, S.E., and Varghese, S.A. (2017). Topical timolol promotes healing of chronic leg ulcer. J. Vasc. Surg. Venous Lymphat.Disord. *5*, 844–850. https://doi.org/10.1016/j.jvsv.2017.04.019.

Todde, S., Moresco, R.M., Simonelli, P., Baraldi, P.G., Cacciari, B., Spalluto, G., Varani, K., Monopoli, a., matarrese, m., carpinelli, a., et al.

(2000). design, radiosynthesis, and biodistribution of anew potent and selective ligand for in vivo imaging of the adenosine A $_{2A}$ receptor system using positron emission tomography. J. Med. Chem. *43*, 4359–4362. https://doi.org/10.1021/jm0009843.

Vaniotis, G., Glazkova, I., Merlen, C., Smith, C., Villeneuve, L.R., Chatenet, D., Therien, M., Fournier, A., Tadevosyan, A., Trieu, P., et al. (2013). Regulation of cardiac nitric oxide signaling by nuclear β-adrenergic and endothelin receptors. J. Mol. Cell. Cardiol. *62*, 58–68. https://doi.org/10.1016/j.yjmcc.2013.05.003.

Velmurugan, B.K., Baskaran, R., and Huang, C.-Y. (2019). Detailed insight on β-adrenoceptors as therapeutic targets. Biomed.Pharmacother. *117*, 109039. https://doi.org/10.1016/j.biopha.2019.109039.

Vickerman, B.M., Zywot, E.M., Tarrant, T.K., and Lawrence, D.S. (2021). Taking phototherapeutics from concept to clinical launch. Nat. Rev. Chem *5*, 816–834. https://doi.org/10.1038/s41570-021-00326-w.

Wachter, S.B., and Gilbert, E.M. (2012). Beta-adrenergic receptors, from their discovery and characterization through their manipulation to beneficial clinical application. Cardiology *122*, 104–112. https://doi.org/10.1159/000339271.

Wang, J., Pani, B., Gokhan, I., Xiong, X., Kahsai, A.W., Jiang, H., Ahn, S., Lefkowitz, R.J., and Rockman, H.A. (2021). *β* -Arrestin–Biased allosteric modulator potentiates carvedilol-stimulated *β*adrenergic receptor cardioprotection. Mol. Pharmacol. *100*, 568–579. https://doi.org/10.1124/molpharm.121.000359.

Wang, Y., Lin, W.K., Crawford, W., Ni, H., Bolton, E.L., Khan, H., Shanks, J., Bub, G., Wang, X., Paterson, D.J., et al. (2017). Optogenetic control of heart rhythm by selective stimulation of cardiomyocytes derived from pnmt+ cells in murine heart. Sci. Rep. *7*, 40687. https://doi.org/10.1038/srep40687.

Warne, T., Edwards, P.C., Leslie, A.G.W., and Tate, C.G. (2012). Crystal structures of a stabilized β1-adrenoceptor bound to the biased agonists bucindolol and carvedilol. Structure *20*, 841–849. https://doi.org/10.1016/j.str.2012.03.014.

Weinrich, T., Gränz, M., Grünewald, C., Prisner, T.F., and Göbel, M.W. (2017). Synthesis of a cytidine phosphoramidite with protected nitroxide spin label for EPR experiments with RNA. European J. Org. Chem. *2017*, 491–496. https://doi.org/10.1002/ejoc.201601174.

Westphal, M.v., Schafroth, M.A., Sarott, R.C., Imhof, M.A., Bold, C.P., Leippe, P., Dhopeshwarkar, A., Grandner, J.M., Katritch, V., Mackie, K., et al. (2017). Synthesis of photoswitchable Δ ^{9} -tetrahydrocannabinol derivatives enables optical control of cannabinoid receptor 1 signaling. J. Am. Chem. Soc. *139*, 18206–18212. https://doi.org/10.1021/jacs.7b06456.

Wisler, J.W., DeWire, S.M., Whalen, E.J., Violin, J.D., Drake, M.T., Ahn, S., Shenoy, S.K., and Lefkowitz, R.J. (2007). A unique mechanism of β-blocker action: carvedilol stimulates β-arrestin signaling. Proc. Natl. Acad. Sci. USA *104*, 16657–16662. https://doi.org/10.1073/PNAS.0707936104.

Wong, G.W., Laugerotte, A., and Wright, J.M. (2015). Blood pressure lowering efficacy of dual alpha and beta blockers for primary hypertension. Cochrane Database Syst. Rev.

https://doi.org/10.1002/14651858.CD007449.pub2.

Xu, X.-L., Zang, W.-J., Lu, J., Kang, X.-Q., Li, M., and Yu, X.-J. (2006). Effects of carvedilol on M2 receptors and cholinesterase-positive nerves in adriamycin-induced rat failing heart. Auton. Neurosci. *130*, 6–16. https://doi.org/10.1016/j.autneu.2006.04.005.

STAR★METHODS

KEY RESOURCES TABLE

REAGENT or RESOURCE	SOURCE	IDENTIFIER
Chemicals, peptides, and recombinant proteins		
Carvedilol	Tokyo Chemical Industry Co., Ltd. (TCI)	Cat#C2260
Isoprenaline hydrochloride	Sigma-Aldrich	Cat#I5627
Cimaterol	Sigma-Aldrich	Cat#32568
Experimental models: Cell lines		
Human: HEK293-H188 M1	(Duran-Corbera et al., 2020)	N/A
Experimental models: Organisms/strains		
Wild-type zebrafish	Exopet	N/A
Mouse: C57BL/6J	INVIGO	N/A
Software and algorithms		
ChemDraw Professional 18.0	PerkinElmer	https://www.perkinelmer.com/category/chemdraw
GraphPad Prism 8.1.1	GraphPad Software	www.graphpad.com
Matlab R2010b	MathWorks	https://www.mathworks.com/products/matlab.html
Mnova 14	Mestrelab	https://mestrelab.com/software/mnova/
Mass Lynx 4.1	Waters	
Ethovision XT 13 software	Noldus	https://www.noldus.com/ethovision-xt
BIOVIA Discovery Studio v20.1.0	Dassault Systèmes	https://www.3ds.com/products-services/biovia/products/molecular-modeling-simulation/biovia-discovery-studio/
uEye Cockpit	IDS Imaging Development Systems	https://es.ids-imaging.com/ids-software-suite.html
Chart 5.0	AdInstruments	N/A
Other		
CoolLED pE-4000 light system	CoolLED	https://www.coolled.com/products/pe-4000/
LEDA Array Teleopto	Teleopto	http://www.teleopto.com/teleopto/led-array-system
HPLC: Thermo Ultimate 3000SD	Thermo Scientific Dionex	https://www.thermofisher.com/es/es/home/industrial/chromatography/liquid-chromatography-lc.html
Mass Spectrometer: LTQ XL ESI-ion trap	Thermo Scientific	https://www.thermofisher.com/order/catalog/product/IQLAAEGAAVFACZMAIK
Tecan Spark M20 multimode microplate reader	Tecan	https://lifesciences.tecan.com/multimode-plate-reader
Motic SMZ-171 dissecting microscope	Motic	https://moticeurope.com/en/microscope/serie/smz171
GigE camera	IDS Imaging Development Systems	https://en.ids-imaging.com/gige-cameras.html
Danio Vision	Noldus	https://www.noldus.com/daniovision
ML119 PowerLab interface	AdInstruments	N/A

RESOURCE AVAILABILITY

Lead contact

Further information and requests for resources and reagents should be directed to and will be fulfilled by the lead contact, Xavier Rovira (xavier.rovira@iqac.csic.es).

Materials availability

All unique and stable reagents generated in this study are available from the lead contact with a completed Materials Transfer Agreement.

Data and code availability

- All data reported in this article will be shared by the lead contact on request.
- All original code is available in this article's supplemental information.
- Any additional information required to reanalyze the data reported in this article is available from the lead contact on request.

EXPERIMENTAL MODEL AND SUBJECT DETAILS

Cell lines

In vitro assays were carried out using a reported HEK-293 cell line stably expressing the Epac-SH[188] biosensor (Duran-Corbera et al., 2020). These cells were maintained at 37°C, 5% CO_2 in 4.5 g/L D-glucose Dulbecco's Modified Eagle Medium (DMEM, GIBCO) supplied with 10% heat inactivated FBS (GIBCO) and 1% penicillin-streptomycin (10,000 U/mL, GIBCO). Cells were split when reaching 75–90% confluence and detached by trypsin digestion.

Mice for *ex vivo* assays

Adult female C57BL/6J mice (25–30 g, 9–11 weeks old) were anesthetized with sodium pentobarbital (1.5 g/kg, I.P.) and submitted to a bilateral thoracotomy. Whole hearts were quickly excised and retrogradely perfused through the aorta with an oxygenated (95% O_2: 5% CO_2) Krebs solution at 37°C (118 mM NaCl, 4.7 mM KCl, 1.2 mM $MgSO_4$, 1.8 mM $CaCl_2$, 25 mM $NaHCO_3$, 1.2 mM KH_2PO_4, and 11 mM glucose, pH 7.4) in a constant flow Langendorff system. Flow was initially adjusted to produce a perfusion pressure of 80–90 mmHg (normoxic conditions). The study was performed according to the Spanish Policy for Animal Protection RD53/2013, which meets the European Union Directive, 2010/63/UE and the NIH Guide for the Care and Use of Laboratory Animals (NIH publications N°. 85-23, revised 1996, updated in 2011). Experimental procedures were approved by the Ethics Committee on Animal Research (CEEA) of the Vall d'Hebron Research Institute (reference 22/20 CEEA).

Zebrafish larvae for *in vivo* assays

Adult wild-type zebrafish, purchased from Exopet (Madrid, Spain), were maintained in fish water (reverse-osmosis purified water containing 90 μg/mL of Instant Ocean (Aquarium Systems, Sarrebourg, France) and 0.58 mM $CaSO_4 \cdot 2H_2O$) at 28 ± 1°C in the animal facilities of the Research and Development Center (CID-CSIC) under standard conditions. Embryos obtained by in-tank group breeding (3:2 female:male ratio) were collected and maintained in 500 mL glass containers at 1 individual/mL density in fish water. Animals were kept at 28.5°C on a 12 light:12 dark photoperiod. Larvae were not fed before or during the experimental period. Seven days post-fertilization larvae were used to evaluate the light dependent potential of caged-carvedilol in living animals. All procedures were approved by the Institutional Animal Care and Use Committees at the CID-CSIC and conducted in accordance with the institutional guidelines under a license from the local government (agreement number 11336).

METHOD DETAILS

Synthesis and compound characterization

All starting materials were obtained from commercial sources and used without further purification unless otherwise stated. Reactions were monitored by TLC on silica gel (60F, 0.2 mm, ALUGRAM Sil G/UV254 Macherey-Nagel) and visualized with 254 nm UV light. Flash column chromatography was carried out using

silica-gel 60 (Panreac, 40–63 μm mesh). Analytical HPLC was performed on a Thermo Ultimate 3000SD (Thermo Scientific Dionex) coupled to a PDA detector and Mass Spectrometer LTQ XL ESI-ion trap (Thermo Scientific); HPLC columns used were ZORBAX Eclipse Plus C18 (4.6 × 150mm; 3.5μm). HPLC purity was determined using the following binary solvent system: 5% ACN in 0.05% formic acid for 0.5 min, from 5 to 100% ACN in 5 min, 100% ACN for 1.5 min, from 100 to 5% ACN in 2 min and 5% ACN for 2 min. The flow rate was 0.5 mL/min, column temperature was fixed to 35°C and wavelengths from 210–600 nm were registered. The purity of all compounds was determined to be >95%. NMR spectroscopy was performed using a Varian-Mercury 400 MHz spectrometer. Chemical shifts are reported in δ (ppm) relative to an internal standard (non-deuterated solvent signal). The following abbreviations have been used to designate multiplicities: s, singlet; d, doublet; t, triplet; q, quadruplet; m, multiplet; br, broad signal; dd, doublet of doublet. Coupling constants (J) are reported in Hz. HRMS and elemental composition were performed on a FIA with Ultra-high-Performance Liquid Chromatography (UPLC) Aquity (Waters) coupled to LCT Premier Orthogonal Accelerated Time of Flight Mass Spectrometer (TOF) (Waters). Data from mass spectra was analyzed by electrospray ionization in positive and negative mode using Mass Lynx 4.1 Software (Waters). Spectra were scanned between 50 and 1500 Da with values every 0.2 s and peaks are reported as m/z.

7-(Diethylamino)-2-oxo-2H-chromene-4-carbaldehyde (**1**): Selenium dioxide (7.10 g, 63.9 mmol) and 7-(diethylamino)-4-methyl-2H-chromen-2-one (5.10 g, 22.05 mmol) were suspended in xylene (315 mL). The reaction mixture was heated to reflux and stirred vigorously for 5 days under an argon atmosphere. The mixture was then filtered through celite and concentrated under reduced pressure to yield aldehyde **1** (5.2 g, 96% yield) as a dark oil. ^{1}H NMR (400 MHz, chloroform-*d*) δ = 10.02 (s, 1H), 8.29 (d, J = 9.2 Hz, 1H), 6.62 (dd, J = 9.2, 2.6 Hz, 1H), 6.51 (d, J = 2.6 Hz, 1H), 6.45 (s, 1H), 3.42 (q, J = 7.1 Hz, 4H), 1.21 (t, J = 7.1 Hz, 6H). The described NMR is in good agreement with the data reported in the literature (Goegan et al., 2018).

7-(Diethylamino)-4-(hydroxymethyl)-2H-chromen-2-one (**2**): A solution of **1** (3.5 g, 14.27 mmol) in methanol (30 mL) was cooled down in an ice bath. Sodium borohydride (540 mg, 14.27 mmol) was then added slowly and the reaction was left to stir overnight. Water (200 mL) was added and the solution was neutralized using 1N HCl. The brown aqueous solution was extracted using EtOAc (3 x 250 mL). The organic phases were poured together, washed with brine and dried over Na_2SO_4. The solvent was removed in vacuo to yield **2** (3 g, 85% yield) as a brown oil. ^{1}H NMR (400 MHz, chloroform-*d*) δ = 7.32 (d, J = 9 Hz, 1H), 6.57 (dd, J = 9, 2.6 Hz, 1H), 6.51 (d, J = 2.6 Hz, 1H), 6.26 (t, J = 1.3 Hz, 1H), 4.83 (d, J = 4.7 Hz, 2H), 3.41 (q, J = 7.1 Hz, 4H), 1.20 (t, J = 7.1 Hz, 6H). The NMR spectrum is in good agreement with that reported in the literature (Schönleber et al., 2002).

4-(Bromomethyl)-7-(diethylamino)-2H-chromen-2-one (**3**): Triethylamine (0.789 mL, 5.66 mmol) was added to a solution of **2** (700 mg, 2.83 mmol) in DCM (12 mL) and the mixture was cooled down in an ice bath. Methanesulfonyl chloride (486 mg, 4.25 mmol) was added dropwise and the reaction was stirred for 2 h. The mixture was quenched with saturated $NaHCO_3$ (25 mL). The organic solution was isolated, dried over Na_2SO_4 and concentrated under vacuum. The obtained crude product was dissolved in THF (12 mL) and treated with LiBr (983 mg, 11.32 mmol). The reaction was concentrated after 2 h, DCM was added and the solution was washed with brine, dried over Na_2SO_4 and concentrated under vacuum. **3** (230 mg, 26% yield) was isolated as a brown solid. ^{1}H NMR (400 MHz, chloroform-*d*) δ = 7.50 (d, J = 8.8 Hz, 1H), 6.64 (d, J = 8.8 Hz, 1H), 6.53 (s, 1H), 6.14 (s, 1H), 4.40 (s, 2H), 3.42 (q, J = 7.1 Hz, 4H), 1.22 (t, J = 7.1 Hz, 6H). The described NMR is in good agreement with the data reported in the literature (Weinrich et al., 2017).

4-(((3-((9H-Carbazol-4-yl)oxy)-2-hydroxypropyl)(2-(2-methoxyphenoxy)ethyl)amino)methyl)-7-(diethylamino)-2H-chromen-2-one (Caged-Carvedilol, **4**): 1-((9H-Carbazol-4-yl)oxy)-3-((2-(2-methoxyphenoxy)ethyl)amino) propan-2-ol (260 mg, 0.640 mmol) was dissolved in DMF (1.5 mL). 4-(Bromomethyl)-7-(diethylamino)-2H-chromen-2-one (198 mg, 0.640 mmol) and triethylamine (90 μL, 0.640 mmol) were added and the mixture was stirred at room temperature for 24h. The solvent was removed under reduced pressure. DCM (20 mL) was added and the organic solution was washed with brine, dried and concentrated under vacuum to yield a brown solid. The crude product was further purified by silica gel column chromatography (DCM:AcOEt,95:5) to yield 250 mg (62% yield) of Caged-Carvedilol (**4**).
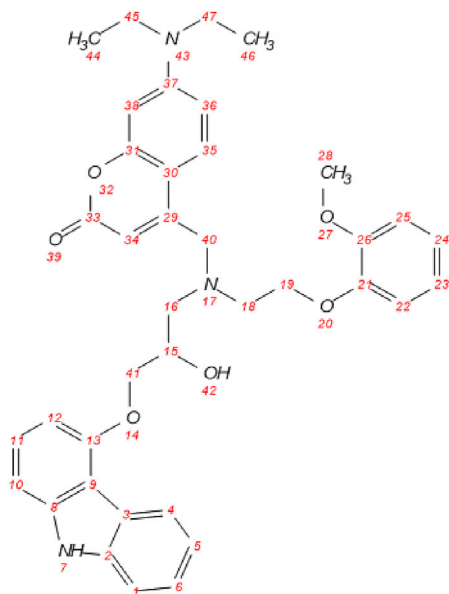
^{1}H NMR (400 MHz, DMSO-d_6) δ 11.20 (s, 1H, H1), 8.17 (d, *J* = 8 Hz, 1H, H4), 7.64 (d, *J* = 9.2 Hz, 1H, H35), 7.41 (d, *J* = 8.0 Hz, 1H, H1), 7.28 (td, *J* = 8.0 and 1.2, 1H, H6), 7.20 (t, *J* = 8.0 Hz, 1H, H11), 7.04 (d, 1H, 8 Hz, 1H, H12), 7.03 (t, *J* = 8 Hz, 1H, H5), 6.91 (dd, *J* = 8, 1.6 Hz, 1H, H25), 6.85 (td, *J* = 7.8, 2.5 Hz, 1H, H24), 6.81 (dd, *J* = 8, 2 Hz, 1H, H22), 6.77 (td, *J* = 8.0 and 1.2, 1H, H23), 6.48 (d, *J* = 8 Hz, 1H, H10), 6.40 (d, *J* = 2.5 Hz, 1H, H38), 6.28 (s, 1H, H34), 6.20 (dd, *J* = 9.2, 2.5 Hz, 1H, H36), 5.06 (d, *J* = 4.8 Hz, 1H, H42), 4.32–4.14 (m, 2H, H15 and H19a), 4.12-4.03 (m, 3H, H19b and H41), 4.00 (d, *J* = 15.2 Hz, 1H, H40a), 3.92 (d, *J* = 15.2 Hz, 1H, H40b), 3.66 (s, 3H, H28), 3.31 (q, *J* = 7.2 Hz, 4H, H45 and H47), 3.03-2.97 (m, 3H, H16 and H18a), 2.87 (dd, *J* = 13.2, 6 Hz, 1H, H18b), 1.04 (t, *J* = 7.2 Hz, 6H (H44 and H46). **^{13}C NMR** (101 MHz, DMSO-d_6) δ 161.0 (C33), 155.8 (C31), 155.0 (C13), 154.0 (C37), 150.0 (C29), 149.0 (C26), 147.9 (C21), 141.0(C8), 138.9 (C2), 126.3 (C11), 126.3 (C35), 124.4 (C6), 122.4 (C4), 121.7 (C3), 120.8 (C24), 120.6 (C23), 118.5 (C5), 112.8 (C22), 111.9 (C25), 111.5 (C9), 110.3 (C1), 108.1 (C36), 107.8 (C34), 107.1 (C30), 103.7 (C12), 100.1 (C10), 96.5 (C38), 70.3 (C19), 67.7 (C15), 66.2 (C41), 57.5 (C18), 56.6 (C40), 55.3 (C28), 53.2 (C16), 43.9 (C45 and C47), 12.3 (C44 and C46). **HRMS (ESI+):** *m/z* calcd for $C_{38}H_{42}N_3O_6^+$ [M + H]$^+$ = 636.3074; found 636.3073.

Molecular modeling

Structures of β$_1$-AR (PDB id: 4AMJ) (Warne et al., 2012) and β$_2$-AR (PDB id: 6PS3) (Ishchenko et al., 2019) in complex with the drug carvedilol were used to place the caged version described in this study. Briefly, the co-crystalized carvedilol of each structure was isolated and modified to include the coumarinyl group. To conserve all important interactions of carvedilol with the receptor, only the coumarinyl group of the molecule was minimized several times using a Dreiding-like forcefield included in the Biovia software suite (BIOVIA, Dassault Systèmes, Discovery Studio, v20.1.0.19295, San Diego: Dassault Systèmes, 2019). The minimized molecule was placed in the same location as the original carvedilol and the unfavorable interactions as well as the bumps were monitored using the computational tool of the Biovia software suite.

Photochemistry

UV-Vis characterization

UV-Vis spectra were recorded using a Tecan Spark 20M Multimode Microplate reader. All samples were prepared with 50 μM of carvedilol, caged-carvedilol and Br-DEACM in PBS (30% DMSO). Samples were measured between 600 and 250 nm with 2 nm fixed intervals in 96-well transparent plates (200 μL of compound solution/well). Illumination was applied from top in continuous mode using the CoolLED pE-4000 light source, set at 5% intensity. CoolLED set at 5% intensity for 405 nm corresponded to 0.51 mW/mm^2 (potency measured using a Thorlabs PM100D power energy meter connected to a standard photodiode power sensor (S120VC)).

Uncaging quantification

Uncaging was monitored by HPLC-MS. Calibration standard curves of carvedilol (concentrations ranging from 0.2–10 μM) and of its caged analogue (4) (2–15 μM) were performed to be able to calculate the concentration of the two species in uncaging assays. The stock solutions of the compounds (10 mM) were diluted 1:100 with water (100 μM final concentration). For carvedilol, an intermediate solution was prepared by 1:2 dilution with water, leading to a 50 μM solution. Using this working solution, intermediate dilutions were prepared in the range of 5–25 μM and these were further diluted in water to the desired concentrations for the calibration curve (0.2–10 μM). To prepare the calibration curve of caged-carvedilol (4), the 100 μM solution was subsequently diluted to intermediate working solutions in the range of 20–75 μM, which were used to prepare the calibration curve solutions. All samples were analyzed by HPLC-MS and calibration curves analyzed.

A 100 μM caged-carvedilol solution (10% DMSO) was illuminated for the studied times. The sample was thereafter diluted to 10 μM in water (1% DMSO) and analyzed by HPLC-MS. Analytical HPLC was performed on a Thermo Ultimate 3000SD (Thermo Scientific Dionex) coupled to a PDA detector and Mass Spectrometer LTQ XL ESI-ion trap (Thermo Scientific). The ESI source was set in positive mode for these experiments. Chromatographic separations were performed using a ZORBAX Eclipse Plus C18 (4.6 × 150mm; 3.5μm) column with the following binary solvent system: from 23 to 30% ACN in 0.05% formic acid for 3 min, from 30 to 35% ACN in 2 min, from 35 to 100% ACN in 1 min, 100% ACN for 2 min, from 100 to 23% ACN in 1 min and 23% ACN for 2 min. The flow rate was 0.9 mL/min, column temperature was fixed to 35°C and wavelengths from 210–600 nm were registered. Quantification was performed using single reaction monitoring (SRM) mode with the transition of m/z 407.3 → 222.1 ± 2, 224.1 ± 2 and 283.1 ± 2 for carvedilol, m/z 658.1 → 423 ± 26, 475 ± 2, 513.5 ± 19, 534.3 ± 2, 590.6 ± 2, 640.4 ± 2 and 654.4 ± 2 for C-C. The optimal source parameters were as follows: sheath gas flow 60, aux gas flow 10, sweep gas flow 10, capillary temperature 300°C, source voltage 3 kV, capillary voltage 42 V and tube lens 110 V. The compound dependent parameter normalized collision energy (CE) was set at 20% for both compounds. The compound dependent parameter normalized Act Q was set at 0.25% for the two compounds. The compound dependent parameter Act Time was set at 30 ms for carvedilol and C-C.

Cell culture and transfection

HEK-293 cells, which endogenously express β$_2$-AR were transfected with the Epac-SH[188] biosensor (1 μg H188 DNA) from Kees Jalink group (Netherlands Cancer Institute) using X-tremeGENE 9 (Sigma-Aldrich, 3:1 X-tremeGENE/DNA ratio) as a transfecting agent. Transfection was carried in 6-well Clear TC-treated Multiple Well Plates (Corning) at a density of 500,000 cells/well. Cells were left to grow for 48h before the selection process was started. The medium was then changed to complete DMEM containing 0.5 mg/mL of Geneticin to only select transfected cells containing the Neomycin resistant gene from the plasmid. Two weeks after, cells were passaged and diluted in decreasing densities in a transparent 96-well plate (limited dilution cloning) using cell culture medium enriched with 0.5 μg/mL of G-418. Single cell colonies were isolated from this process, grown, and their functional activity was assessed with the agonist cimaterol. Cells obtained following this protocol, named HEK293-H188 M1, were used thereafter to evaluate the functional activity of β$_2$-AR. Cells were maintained at 37°C, 5% CO$_2$ in 4.5 g/L D-glucose Dulbecco's Modified Eagle Medium (DMEM, GIBCO) supplied with 10% heat inactivated FBS (GIBCO) and 1% penicillin-streptomycin (10,000 U/mL, GIBCO). Cells were split when reaching 75–90% confluence and were detached by trypsin digestion.

Pharmacology

All assays were performed at room temperature. Adherent cells were grown in T-175 flasks or 150-mm dishes to 75–90% confluence. Cells were detached by rinsing once with PBS (GIBCO), followed by incubation with Trypsin-EDTA (Sigma-Aldrich) for 5 min until detachment of cells was observed. Cells were then centrifuged; in parallel, 10 μL of the single cell suspension were counted using a Neubauer Chamber. The supernatant was carefully removed, and cells were resuspended in DMEM complete medium to obtain a cell solution with 1.0 x 10^6 cells/mL. 100,000 cells per well were seeded in a transparent 96-well microplate (Thermo Scientific Nunc MicroWell) and left at 37°C with 5% CO$_2$ for approximately 24 h (Duran-Corbera et al., 2020). cAMP EPAC sensor buffer (14 mM NaCl, 50 nM KCl, 10 nM MgCl2, 10 nM CaCl2, 1 mM N-(2-hydroxyethyl)piperazine-N'-ethanesulfonic acid (HEPES), 1.82 mg/mL glucose, pH 7.2) supplemented with 100 μM IBMX was used as assay medium in all FRET-based experiments. 10 μM aliquots of caged-carvedilol were pre-illuminated at the different studied times using the CoolLED pE-4000 light source, set at

10% intensity. The differently illuminated caged-carvedilol samples were pre-incubated with the cells for 15 min. The agonist cimaterol was then added (3 nM) and the plate was incubated for 30 min more. For the time course experiments in cell cultures, both the agonist (cimaterol) and the C-C were added at the same time. The effect of the agonist (3 nM) with carvedilol at 100nM was also measured and later used for data normalization. For the illumination pulses, external light was applied using the 96-well LED array plate (LEDA Teleopto) at 405 nm and the sample was rapidly introduced into the plate reader to continue the activity monitorization. Fluorescence values were measured using a Tecan Spark M20 multimode microplate reader programmed with the following wavelength settings: excitation filter 430/20 nm and emission filters 485/20 nm and 535/25 nm. FRET ratios were calculated as the relation of the donor emission (td^{cp173}V, 485 nm) divided by the acceptor emission (mTurq2Δ, 535 nm). The obtained ratios were normalized to the effect of the agonist cimaterol (100%) and the minimum response obtained with the antagonist carvedilol (0%). Each set of experiments was performed three times with each concentration in duplicate. These experiments were analyzed using GraphPad Prism 8.1.1 (GraphPad Software, San Diego, CA). Inhibition dose-response data was fitted using the log(antagonist) vs. response (three parameters) function. Data is shown as the mean $\pm$ SEM of the three experiments.

Langendorff heart experiments

Perfused mice hearts were used to evaluate the light dependent effects over the cardiac rhythm of the caged beta blocker. Left ventricular (LV) pressure was monitored with a water-filled latex balloon connected to a pressure transducer, placed in the left ventricle and inflated to obtain an LV end-diastolic pressure (LVEDP) between 6 and 8 mmHg. Perfusion pressure was monitored through a lateral access into the cannula. All signals were recorded in a computer using an ML119 PowerLab interface and Chart 5.0 software (AdInstruments, Castle Hill, Australia). After 35 min of equilibration, isolated mice hearts were treated with normoxic Krebs or with Krebs containing 25 µM C-C, or 25 µM of illuminated C-C (405 nm, 2 × 2.5 min) for 40 min. In addition, 100 nM isoprenaline was simultaneously included into the corresponding Krebs solution, and administered to all hearts during the last 10 min. Changes in heart rate were continuously monitored for an additional 30 min. Three to five mice hearts were used for each experimental condition tested. Variations on the measured heart beat over the course of the experiment were represented as the mean $\pm$ SEM of the independent replicates using GraphPad Prism.

Assays in zebrafish larvae

Behavioral studies

7 days post fertilization (dpf) larvae were used for all experiments. Exposures were conducted in 48-well microplates containing 1 larva per well and 1 mL of working solution (total 48 larvae per plate). After 1 h of exposure at 28.5°C (POL-EKO APARATURA Climatic chamber KK350, Poland), behavior was directly tested without further manipulation. Behavioral assays were performed using a Danio Vision system running an Ethovision XT 13 software (Noldus, Wageningen, the Netherlands). Larvae were acclimated in the dark for 10 min before video recording. Video tracking conditions included a further 10 min cycle under dark conditions followed by a 50-s stimulus period, which consisted of the delivery of 50 tapping stimuli, one every second. Tapping stimulus was selected at the highest intensity (intensity level: 8). Trials were performed at 28°C with near-infrared light and videos were recorded at 30 frames per second and the responses were analyzed using the EthoVision XT 13 software (Noldus, Wageningen, the Netherlands). The basal locomotor activity (BLA) is defined as the total distance (cm) traveled by the larvae during a period of 10 min of under dark conditions. This parameter was analyzed for each individual larva from the 10 min video tracking (Faria et al., 2015, 2020). The Vibrational Startle Response (VSR) assay is based on the escape response evoked in zebrafish larvae by a tapping stimulus. VSR was analyzed for each individual larva by measuring the distance traveled (cm) over the 1 s period following each stimulus. The VSR assay allows us to obtain two behavior responses: The "Startle Response" and the "Habituation". The startle response is defined as the total distance moved (cm) in response to the first stimulus. Distance values for each individual were normalized to the average distance of the control group (100%) and no movement (0%). Results are represented in a bar chart as the mean $\pm$ SEM of all the individuals tested. The habituation evaluates a form of non-associative learning, defined as the area under the curve (AUC) of plots of distance moved by larvae during the delivery of 50 consecutive tapping stimuli relative to the response to the first stimulus. The distance traveled by each larva after every tapping stimulus applied, was normalized for each experimental group and replicate independently. The mean startle response for each group was used to determine the maximal response (100%), and 0% was attributed to no movement. The habituation profile was represented as the mean normalized distance for each tapping stimulus of three independent

replicates (Faria et al., 2020). The total area under the curve (AUC), extracted from the habituation profile, is represented as the mean $\pm$ SEM of the three independent experiments.

Heart rate monitorization

Seven dpf larvae were used to assess the effects of the caged compound on the cardiac output of living animals. Exposure to the different compounds were conducted for 1 h at 28.5°C (POL-EKO APARATURA Climatic chamber KK350, Poland). Afterward, zebrafish larvae were observed under a Motic SMZ-171 dissecting microscope fitted with a GigE camera (iDS - Imaging Development Systems GmbH). Heart rates were measured in 8–10 larvae from each experimental condition. Larvae were placed over 3% methylcellulose with a drop of medium water and positioned on the left side, which allowed a good visualization of the heart. Videos were recorded for 30 s using uEye Cockpit application (iDS software) at a frame rate of 40 fps. Videos were then analyzed with a MATLAB script developed in our lab (version R2010b, MathWorks, USA) to obtain heart beats per minute for each individual. The program was based on a code to measure the heart rate over time from a video of a human fingertip captured with a smartphone camera (GitHub: uavster/Video2HeartRate). Briefly, the brightness signal over time of the heart region is computed as pixel variations between frames. Then, a band-pass filter is applied (Butterworth filter) to attenuate all frequencies outside the band of interest and a Fourier transform is calculated using the Fast Fourier Transform (FFT) algorithm to translate the signal from the time domain to the frequency domain. Finally, the maximum FFT amplitude is captured, and the corresponding frequency transformed to beats per minute (BPM). Three independent experiments were performed, with 8–10 animals used in each experimental condition. The cardiac rhythm of each larva tested within an experiment was normalized to the mean cardiac rhythm of the control group (100%), and no beating was attributed to 0%. Data of these experiments are shown as scattered plots, where each point represents a biological replicate and the black line represents the mean value.

QUANTIFICATION AND STATISTICAL ANALYSIS

Data from *in vitro*, *ex vivo*, and *in vivo* experiments was analyzed and represented using GraphPad Prism 8.1.1 (GraphPad Software, San Diego, CA). Experiments were performed at least three independent times and data are always presented as the mean $\pm$ SEM unless otherwise stated in the figure legends. Statistical differences were considered significant when $p < 0.05$ and are represented by asterisks (*$p < 0.05$, **$p < 0.01$, ***$p < 0.001$ and ****$p < 0.0001$).

For the analysis of *in vitro* assays, inhibition Dose-Response data was fitted using the log(antagonist) vs. response (three parameters) function.

Monitorization of the cardiac rhythm in perfused mice hearts was conducted using Chart 5.0 software (AdInstruments, Castle Hill, Australia). Each experimental condition was tested in 3–5 different perfused mice hearts. Statistical analysis of the *ex vivo* experiments was performed by repeated measures ANOVA(MANOVA) and Tukey's *post hoc* test.

Behavioral assays *in vivo* were monitored using an EthoVision XT 13 software. 7 to 15 individuals were included in each group, and experiments were repeated three times. The cardiac frequency in zebrafish larvae was monitored by recording 30 s videos using the uEye Cockpit application. 8-10 seven days post-fertilization larvae constituted each experimental group and the experiment was performed three times. The videos were analyzed with a MATLAB script developed in our lab (version R2010b, MathWorks, USA), which provided the cardiac rhythm (heartbeats per minute) for each individual. Data from each experiment was normalized as described in the method details section. For the statistical analysis of all *in vivo* experiments, one-way ANOVAs followed by Tukey's multiple comparisons tests were performed.